Common Measurements in the Central Nervous System by Computed Tomography and Magnetic Resonance Imaging

Pablo Sartori[1]*, Luis Alvarado[2], María Chirveches[2], Macarena Urrutia[3], Braian Yampolsky[1]

1. Diagnóstico Mediter, Sanatorio Julio Méndez, Ciudad Autónoma de Buenos Aires, Argentina.
2. TCba. Centro de Diagnóstico, Ciudad Autónoma de Buenos Aires, Argentina.
3. Instituto de Investigaciones Neurológicas Dr. Raúl Carrera (FLENI), Ciudad Autónoma de Buenos Aires, Argentina.
*Corresponding author.
Email address: pablomsar@yahoo.com.ar

Abstract: On daily practice, during the making of reports, anatomical variants often appear, as well as injuries and different pathologies of the central nervous system (CNS) in which it is necessary to take some kind of measurements, to make an accurate diagnosis. These measurements allow the practicing physician to program and perform minimally invasive therapeutic methods or others that request a surgery of greater relevance. In this paper, we describe the most common measurements in the CNS by using computed tomography (CT) or magnetic resonance imaging (MRI).

Key words: central nervous system; multidetector computed tomography; magnetic resonance imaging

1. Introduction

The precise knowledge of the anatomy and morphology of the structures that make up the central nervous system (CNS) allows, in daily practice, the preparation of reports with a detailed description, as well as the recognition of anatomical variants and different pathologies that arise. Measurement of these structures under normal conditions allows categorization and recognition of abnormal measurements when they occur. The aim of this paper is to describe and illustrate the most common measurements, providing detailed information to the referring colleagues, collaborating with an accurate diagnosis and providing data that allow choosing the appropriate therapy. The most commonly used measurements in neuroimaging studies are the following.

2. Common Measurements

2.1 Quantification of blood volume

Hemorrhagic cerebrovascular accidents(CVA) is a common cause of emergency department visits, accounting for 10% of all CVA, affecting 37,000.0 patients per year in the United States. [1, 2] The main cause of hemorrhagic CVA is arterial hypertension. [1] The presence of intracerebral bleeding is associated with a 40% mortality rate within one month of occurrence and 60% leads to disability with the need for subsequent permanent care. [1, 2, 3] Knowing the volume of bleeding is a fundamental and determining prognostic factor in its treatment and evolution. It also allows prediction of

morbidity and mortality [1]. The greater the volume of bleeding, the worse the patient's prognosis, especially when associated with neurological impairment. [1]

Generally, neuroradiology reports usually highlight the existence of bleeding, location and laterality, and may expand on the presence of mass effect and associated edema, but do not usually specify the measurements for bleeding volume. The ABC/2 formula constitutes a reliable and accurate value for quantification of bleeding volume to be performed in a multiplanar computed tomography (CT) scan in emergency situations. [1, 2]

ABC/2 method: The measurement of the volume of an intraparenchymal hematoma is performed by using a method called ABC/2, which is based on the calculation of the volume of an ellipsoid or sphere. [2, 4, 5, 6, 7] It was first reported by Kwak. [8]

To implement this method of measuring the volume of intraparenchymal hematomas by brain CT, the slice with the area of greatest bleeding is chosen and the maximum anteroposterior diameter of the slice is measured (parameter A). Parameter B corresponds to the transverse diameter of the lesion in that same slice. [3, 4, 7] Parameter C is the number of slices in which bleeding is seen multiplied by the slice thickness (Fig. 1). [1, 3, 4, 7]
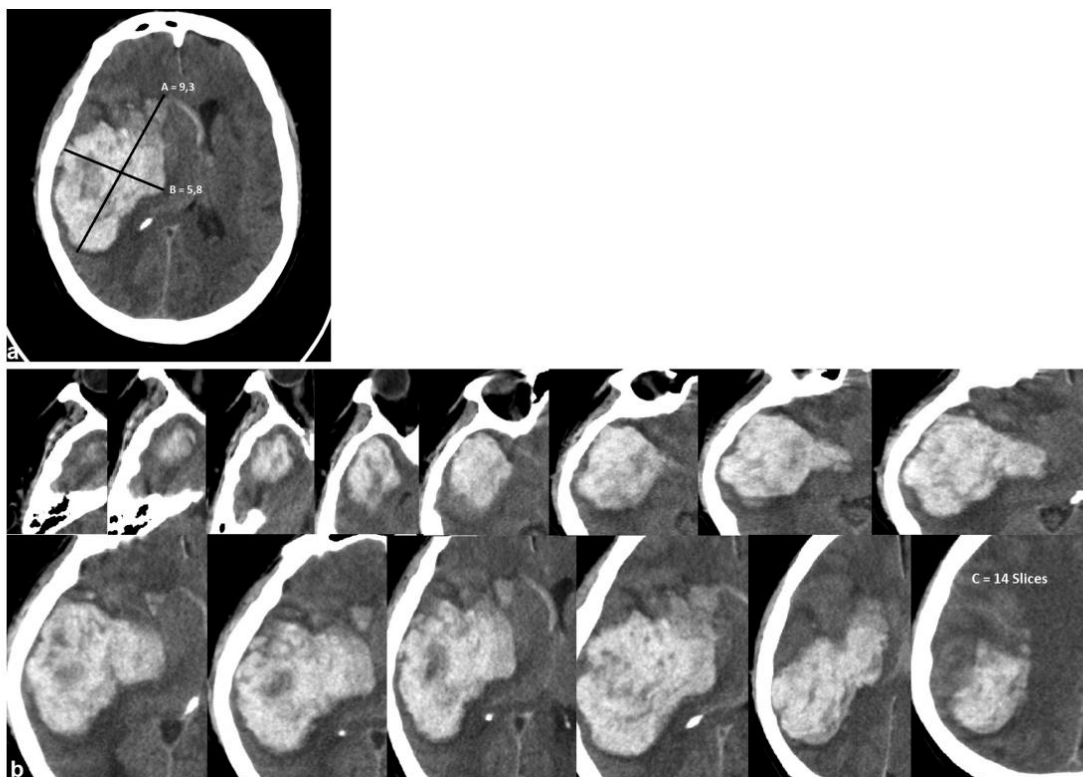

Figure 1. Hematoma measurement.

Hematoma measurement. ABC/2 method. Axial slices are used for this measurement. CT scan of the brain shows a voluminous right fronto-temporo-parietal hematoma, with mass effect displacing the midline and associated ventricular overturning. In (a), the maximum anteroposterior diameter (A = 9.3) and the maximum transverse diameter of the hematoma (B = 5.8) are measured. (b) shows the total number of slices in which bleeding is seen, which would correspond to C = 14 multiplied by the slice thickness 0.5 cm, which would correspond to C = 7. Extrapolating the equation would be: ABC/2: $9.3 \times 5.8 \times 7/2 = 188.7$ cm^3. The formula is: $A \times B \times C /2$ and the final result is expressed in cubic centimeters. [1]

Cohort studies recommend surgical treatment in patients with a bleeding volume greater than 25 cm^3; In cases where the lesion is small, the indication is variable, depending on the patient's clinical condition. [4]

Risk signs of neurological deterioration include intraparenchymal collections greater than 25 cm^3, subdural collections greater than 1 cm^3, increased intracranial pressure, midline shift greater than 5 mm, dilatation of the ventricle contralateral to the hemisphere of the hemorrhagic lesion, obliteration of the meddle cerebral cistern, pericerebral cistern or the III ventricle. [4]

The ABC/2 method allows rapid quantification of the volume of a hematoma without the need for specialized software and can be performed with the patient in the emergency room. However, some authors consider the method not very specific, since it may underestimate the volume of the hematoma, especially in those bleedings with irregular borders, with polylobed contours or that do not have an elliptical shape, and other computer-assisted volumetric (planimetric) techniques that incorporate special software may be considered. [1, 3, 4, 5, 6, 7]

2.2 Midline measurement

The presence of a lesion (intra-axial or extra-axial) with mass effect, can generate midline displacement, causing hernia, compression of basal cisterns, increased intracranial pressure and leading to death. [8, 9]

This displacement can be measured through CT or magnetic resonance imaging (MRI) in an axial slices, referring to the position of the main medial structures, such as the septum pellucidum, cerebral sickle, III ventricle, or pineal gland. [8.9] To measure it, a straight line is drawn that passes through the cerebral sickle and is inserted from its head into the back of the internal table. [9, 10, 11]

In the event that a lesion generates a mass effect and displaces the midline, the aforementioned medial structures will be displaced. To measure this displacement, a line is drawn perpendicular to the midline up to where the septum pellucidum or cerebral sickle is located and the distance from the septum pellucidum or cerebral sickle is measured (Fig. 2). [9, 10, 11]
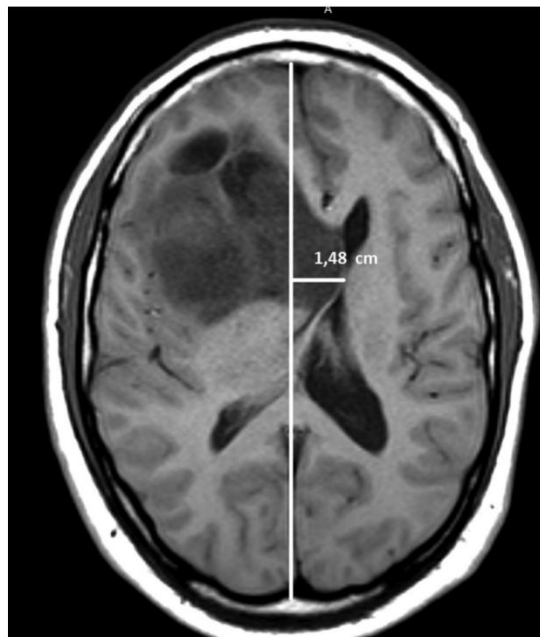

Figure 2. Brain magnetic resonance imaging.

The measurement of the midline is performed through axial slices of CT or MRI. Brain magnetic resonance imaging. T1 weighted axial section showed a mass effect in right frontal glioblastoma, with a median shift of approximately 1.48 cm to the left. A midline displacement greater than 0.5 cm is a predictor of poor prognosis for the neurological outcome of patients with head trauma admitted to intensive care. [12, 13]

2.3 Assessment of cerebellar tonsil protrusion or descent

The cerebellar tonsils are ovoid structures located on the inferior surface of the cerebellum, directly at the head of the foramen occipitalis. They owe their name to their resemblance to almonds. [14] The causes of tonsillar descent are various, including: increased intracranial pressure, myelomeningocele, Chiari malformation, posterior fossa hypoplasia, idiopathic scoliosis, etc. [14]

Ectopia of the cerebellar tonsils is considered as the inferior displacement of the cerebellar tonsils when it is less than or equal to 5 mm. [14, 15] A descent greater than 5 mm is considered a variant of Chiari malformation. [14, 16]

MRI is the modality of choice, with sagittal slices being preferred for measurement, since coronal slices make it difficult to visualize the limits of the foramen magnum. [17] The measurement should be taken by drawing a straight line between the basion and the opisthion of the foramen magnum. Then draw a line perpendicular to the first one, up to the distal end of the herniated tonsil (Fig. 3).
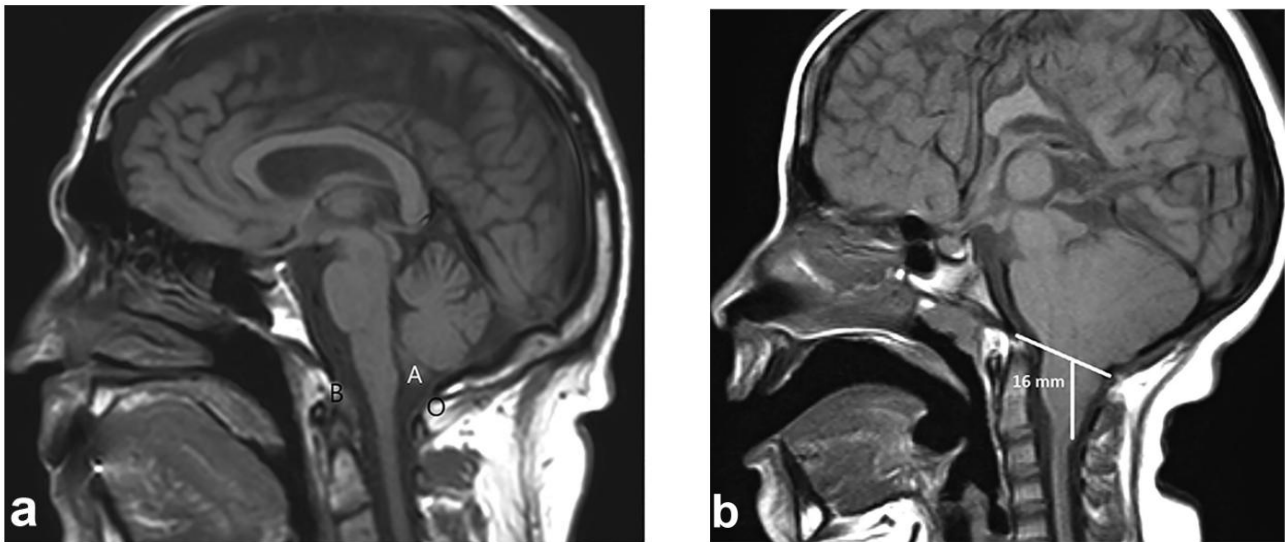

Figure 3. (a) Sagittal slices and (b) MRI of the brain.

(a) Sagittal slices, preferably in MRI, are used to assess tonsillar descent. MRI in T1-weighted sequence of the craniocervical junction. The Basion (B), Opistion (O) and the cerebellar tonsils (a) of normal location are marked. (b) MRI of the brain, and T1-weighted sagittal slice in a patient with Arnold-Chiari II malformation. There is descent of the cerebellar tonsils through the foramen magnum in 16 mm. It was accompanied by syringomyelia (not shown).

There is disagreement among cohort studies regarding the exact value in millimeters of tonsillar descent. Table 1 summarizes the measures of tonsillar descent according to age group. [20]

Table 1. Normal descent of the cerebellar tonsils, according to age [20]

Decade	Decrease in mm considered normal
First	6
Second and third	5
Fourth to eighth	4
Ninth	3

There is a relationship between the degree of tonsillar descent and the presence and degree of symptomatology, [17] and descents of less than 10 mm usually do not cause symptoms. [19]

2.4 Assessment of encephalic atrophy

Both CT and MRI are used for the assessment of standardized measurements to calculate or estimate the evolution of some diseases generally related to movement disorders or dementia. [21, 22]

The bicaudate, Evans and bifrontal indices are obtained in axial CT and MRI slices with orbito-meatal orientation, being used to measure physiological aging and to quantify the degree of brain atrophy (Tables 2, 3 and 4). [22, 23, 24]

Table 2. Normal values of the indexes, distributed by sex (including standard deviation) [22]

Index	Male	Female	Value p*
Bifrontal	0.326 +/- 0.033	0.319 +/- 0.031	> 0.05
Bicaudate	0.132 +/- 0.040	0.119 +/- 0.032	< 0.05
Evans	0.270 +/- 0.026	0.263 +/- 0.026	> 0.05
* The Pearson correlation coefficients obtained between the indexes and age were for the bifrontal index: r = 0.64; for the bicaudate index: r = 0.69 and for the Evans index: r = 0.60.			

Table 3. Normal values of the indexes, distributed by sex in persons under or equal to 50 years of age (including standard deviation) [22]

Index	Male	Female	Average 50 years old	Value p*
Bifrontal	0.308 +/- 0.030	0.310 +/- 0.033	0.309 +/- 0.031	> 0.05
Bicaudate	0.109 +/- 0.020	0.108 +/- 0.022	0.108 +/- 0.021	> 0.05
Evans	0.259 +/- 0.023	0.257 +/- 0.026	0.258 +/- 0.024	> 0.05
* The Pearson correlation coefficients obtained between the indexes and age were for the bifrontal index: r = 0.64; for the bicaudate index: r = 0.69 and for the Evans index: r = 0.60.				

Table 4. Normal values of the indexes, distributed by sex in people over 50 years of age (including standard deviation) [22]

Index	Male	Female	Value p*
Bifrontal	0.343 +/- 0.028	0.327 +/- 0.028	> 0.05
Bicaudate	0.153 +/- 0.043	0.129 +/- 0.036	< 0.05
Evans	0.281 +/- 0.024	0.269 +/- 0.024	> 0.05
* The Pearson correlation coefficients obtained between the indexes and age were for the bifrontal index: r = 0.64; for the bicaudate index: r = 0.69 and for the Evans index: r = 0.60.			

A) Bicaudate index: The minimum distance between the lateral ventricles and the level of the head of the caudate nucleus was divided by the cranial diameter at that level (Fig. 4).
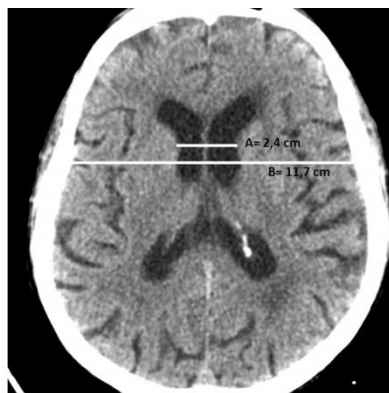

Figure 4. CT axial brain slice.

Measurement of the bicaudate index should be performed with CT or MRI axial slices. CT axial brain slice. A 78-year-old male patient with cognitive impairment. A straight line is drawn measuring the distance between the medial borders of the heads of both caudate nuclei (A = 2.4 cm). Then another line is drawn measuring the maximum cranial diameter at that level (B = 11.7 cm). The formula would be 2.4% × 11.7 = 0.20, indicating moderate atrophy.

B) Evans index: calculated by dividing the maximum diameter of the frontal horns of the lateral ventricles by the maximum intracranial diameter in the same slice at the level of Monro's foramina (Fig. 5). [22, 23, 24]
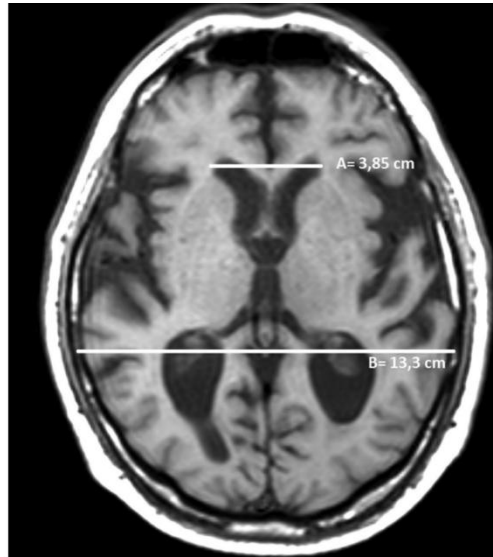

Figure 5. Brain MRI.

The Evans index is obtained in axial slices in both CT and MRI. Brain MRI. Axial slice in T1-weighted sequence. The distance between the frontal extensions of the lateral ventricles (A = 3.85 cm) divided by the maximum diameter of the skull in the same slice at the level of the Monro foramen(B = 13.3 cm) should be measured, exemplifying 3.85% × 13.3 = 0.28 for a 63-year-old patient with incipient intellectual developmental disorder.

A value greater than 0.30 indicates ventricular hypertrophy, which may be considered pathological, but the cause cannot be distinguished by atrophy or other entities. [22, 23, 24]

C) Bifrontal index: it is calculated by dividing the maximum diameter of the frontal horns of the lateral ventricles and the intracranial diameter at the same level (Fig. 6). [22, 23, 24]
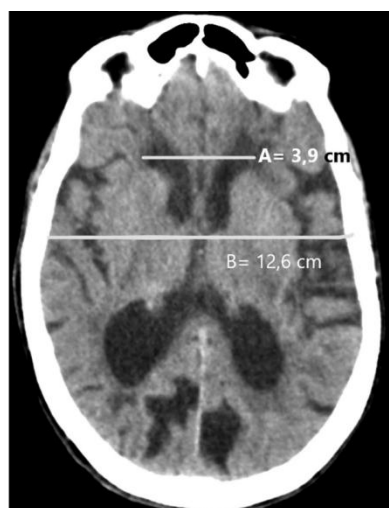

Figure 6. T1-weighted MRI.

The bifrontal index (such as that of Evans), should be obtained in axial CT or MRI slices, as shown in this T1-weighted MRI, in which the distance between the frontal extensions of the lateral ventricles is measured, divided by the maximum intracranial diameter at that level. In our example, it would be: 3.9% × 12.6 = 0.30, indicating a normal value for a 63-year-old patient.

2.5 Cerebral peduncle angle measurement

It is a measure used to quantify the neurodegenerative disease known as Steele-Richardson-Olszewski syndrome (SROS). This pathology is characterized by selective atrophy of the brainstem, especially at the level of the cerebral peduncles, generating increased opening in the interpeduncular cistern assessed in axial CT or MRI sequences. [24]

In an axial slice of a brain MRI, at the level of the mammillary tubercles, two lines are drawn parallel to the medial edges of the cerebral peduncles until they contact at their apex, measuring the angle they form (Fig. 7). [2]
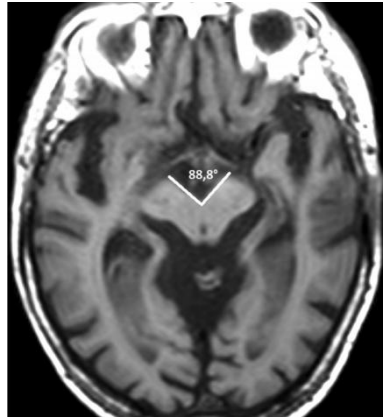

Figure 7. Non-oblique axial CT or MRI slices.

Non-oblique axial CT or MRI slices are used to measure the angle of the cerebral peduncle. Brain MRI, T1-weighted sequence: patient diagnosed with SROS three years ago. The angle of the cerebral peduncle is 88.8°, which is consistent with values for her baseline disease.

A cerebral peduncle angle value greater than or equal to 62° corroborates the diagnosis of SROS, differentiating it from other neurodegenerative pathologies with a lesser degree of openness, such as Parkinson's syndrome (53-54°) or Multiple System Atrophy (55-56°). [24]

2.6 Measurement of the antero-posterior diameter of the midbrain

The reduction of the anteroposterior diameter of the midbrain at the level of the superior quadrigeminal tubercles (colliculi) is characteristic of SROS, giving rise to a typical "Mickey Mouse head" configuration (Fig. 8). [25, 26]
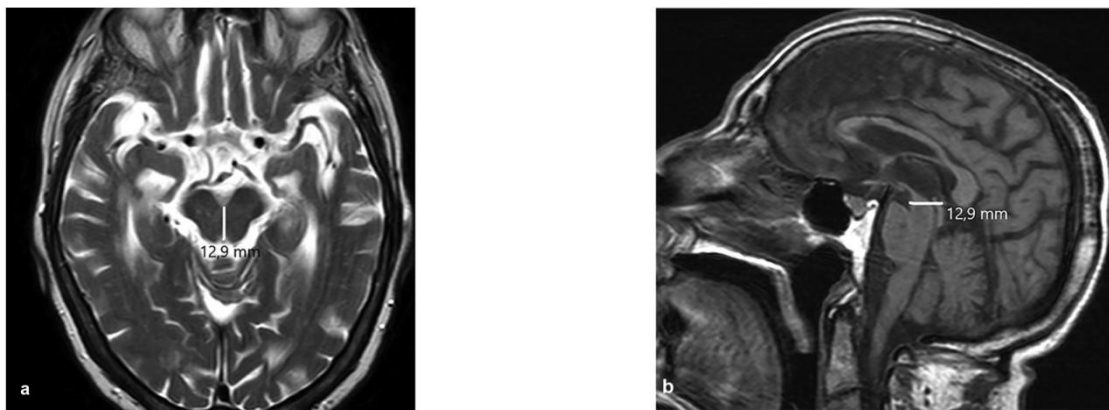

Figure 8. (a) axial T2-weighted views and (b) sagittal T1-weighted views.

The anteroposterior diameter of the midbrain is performed in MRI at the level of the superior colliculi in axial T2-weighted (a) and sagittal T1-weighted (b) views, in a patient with clinical suspicion of SROS. Note the characteristic "Mickey Mouse head" configuration of the midbrain (a). The anteroposterior diameter of the peduncles is 12.9 mm, indicating marked mesencephalic atrophy and confirming the diagnosis of SROS.

This measurement is obtained in axial T2-weighted axial slices or T1-weighted sagittal slices of MRI, drawing a line from the ventral edge of the midbrain, at the level of the superior colliculi, to the dorsal edge. [25] The approximate anteroposterior diameter of the midbrain in patients with SROS is usually less than 14 mm; higher values allow ruling out SROS. [25]

2.7 Assessment of temporal horn width in Alzheimer's disease

There are several imaging parameters to assess the degree of atrophy or involution of the encephalic parenchyma in various neurodegenerative diseases, such as Alzheimer's disease. These measurements are indicators that show disease progression.

There is involution of the encephalic parenchyma at the level of the hippocampal gyrus, amygdala and entorhinal cortex. [21] To assess it, both CT and MRI can be used to measure the width of the temporal horn of the lateral ventricles to compare the progression of the encephalic atrophy in subsequent studies. [21]

The maximum diameter of the temporal horn is measured in an axial CT slice, then the maximum biparietal diameter is taken in the same slice to make the quotient between both measurements (Fig. 9). [21]

Figure 9. Axial CT or MRI slices.

Patient with clinical suspicion of Alzheimer's disease. Axial CT or MRI slices can be used to measure the temporal horn. CT is performed to assess the width of the temporal horn of the lateral ventricles, which measure 7 mm. The maximum intracranial diameter is 122 mm. The ratio between both is 0.05, being compatible with the presumptive diagnosis.

In normal persons, the value is 0.025. In patients with Alzheimer's it is 0.038 and 0.044 in patients with Alzheimer's associated with extensive white matter lesions. [21]

In MRI, a coronal slice (always at the same level) is used to measure the width of the temporal horn (Fig. 10). [21] In a cohort study in patients over 60 years of age they estimated temporal horn values of 6.6 mm in mild Alzheimer's disease and 7.2 mm for advanced. [21]
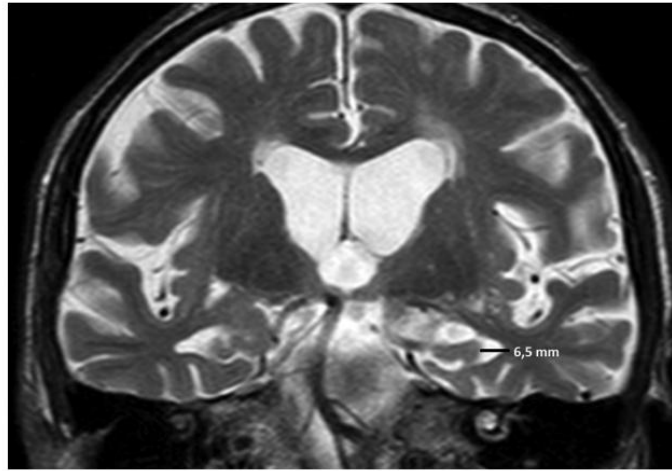
Figure 10. Coronal MRI slices.

Coronal MRI slices allow an accurate measurement of the temporal extension of the lateral ventricle. T2-weighted coronal slice at the level of the temporal extension of the lateral ventricle. The distance of the horn width is 6.5 mm, in relation to mild Alzheimer's disease.

2.8 Proptosis

Proptosis is the anterior displacement or protrusion of the eyeball. The term exophthalmos is used synonymously with proptosis, although it is often associated with endocrine ophthalmopathies. [27] Propotsis can be quantified using axial CT or MRI scans showing the eyeball at its maximum diameters (even prenatally). [27, 28, 28, 29, 30]

For this, a straight line is drawn between the two zygomatic processes (interzygomatic line). Then another line (perpendicular to the interzygomatic line) is drawn towards the posterior sclera: the average normal value is 9.9 +/- 1.7 mm (Fig. 11). [27, 28, 29, 30]
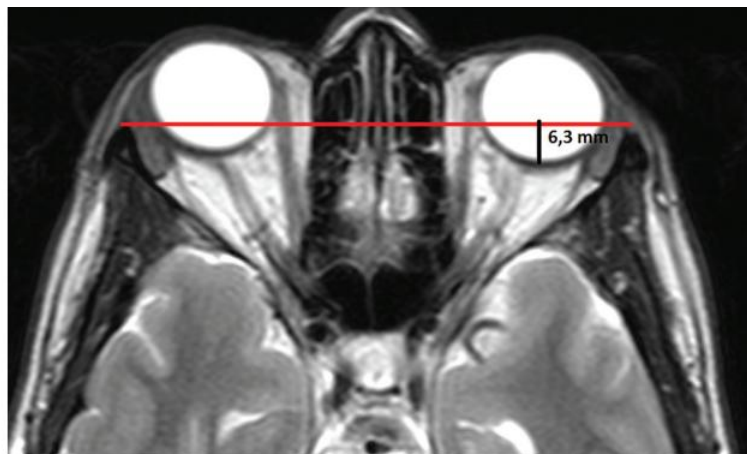

Figure 11. MRI of orbits, T2-weighted axial view.

Both CT and MRI in axial slices at the level of the orbits should be considered to achieve a correct measurement. MRI of orbits, T2-weighted axial view. To assess proptosis, a line should be drawn between the zygomatic processes (red line), then a line perpendicular to the anterior line is drawn up to the posterior sclera (black line). Values greater than 9.9 mm are compatible with proptosis. In our example, the distance is less, so it is considered as normal.

The distance between the interzygomatic line and the anterior border of the eyeball should be less than 21-23 mm (Fig. 12). [27, 28, 29, 30]
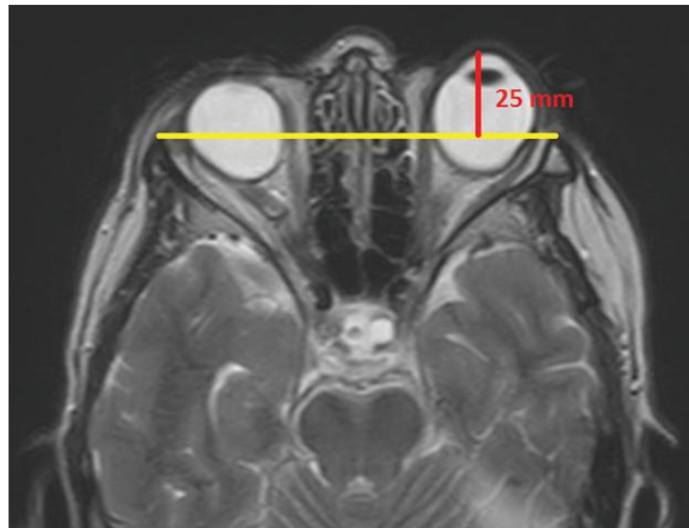
Figure 12. MRI in T2-weighted sequence.

Another way to evaluate if there is proptosis by means of axial CT or MRI slices, is the one shown in this MRI in T2-weighted sequence, in which the interzygomatic line (red line) is made, then another line is drawn perpendicular to it up to the anterior border of the eyeball, being considered normal up to 21-23 mm. Our example exceeds it (25 mm), so there is proptosis.

Conflicts of Interest

The author declares no conflicts of interest regarding the publication of this paper.

References

[1] Maeda AK, Aguiar LR, Martins C, Bichinho GL, Gariba MA. Hematoma Volumes of Spontaneous Intracerebral Hemorrhage: The Ellipse (ABC/2) Method Yielded Volumes Smaller Than Those Measured Using the Planimetric Method. *Arq Neuropsiquiatr*. 2013;71(08):540-544.

[2] Zimmerman RD, Maldjian JA, Brun NC, Horvath B, Skolnick BE. Radiologic Estimation of Hematoma Volume in Intracerebral Hemorrhage Trial by CT Scan. *AJNR Am J Neuroradiol*. 2006;27(03):666-670.

[3] Webb AJ, Ullman NL, Morgan TC, Muschelli J, Kornbluth J, Awad IA, et al; MISTIE and CLEAR Investigators. Accuracy of the ABC/2 Score for Intracerebral Hemorrhage: Systematic Review and Analysis of MISTIE, CLEAR-IVH, and CLEAR III. *Stroke*. 2015;46(09):2470-2476.

[4] Arikan F, Sahuquillo J, Ibáñez J, Vilalta J, Poca MA, Riveiro M, et al. Variabilidad en las indicaciones quirúrgicas de las lesiones intradurales postraumáticas. Neurocirugia (Astur). 2005;16(02):108-116.

[5] Wang CW, Juan CJ, Liu YJ, Hsu HH, Liu HS, Chen CY, et al. Volume-dependent Overestimation of Spontaneous Intracerebral Hematoma Volume by the ABC/2 Formula. Acta Radiol. 2009;50(03):306-311.

[6] Kleinman JT, Hillis AE, Jordan LC. ABC/2: Estimating Intracerebral Haemorrhage Volume and Total Brain Volume, and Predicting Outcome in Children. *Dev Med Child Neurol*. 2011;53(03):281-284.

[7] Hu TT, Yan L, Yan PF, Wang X, Yue GF. Assessment of the ABC/2 Method of Epidural Hematoma Volume Measurement as Compared to Computer-assisted Planimetric Analysis. *Biol Res Nurs*. 2016;18(01):5-11.

[8] Gebel JM, Sila CA, Sloan MA, Granger CB, Weisenberger JP, Green CL, et al. Comparison of the ABC/2 Estimation Technique to Computer-assisted Volumetric Analysis of Intraparenchymal and Subdural Hematomas Complicating the GUSTO-1 Trial. *Stroke*. 1998;29(09):1799-1801.

[9] Liao CC, Chen YF, Xiao F. Brain Midline Shift Measurement and Its Automation: A Review of Techniques and Algorithms. *Int J Biomed Imaging*. 2018;2018:4303161.

[10] Escario JA, Martínez Quiñones JV, Gallego AM, Arregui Calvo R, Suárez Mier MP. Hernias encefálicas. Clasificación, neuropatología y problemas medicolegales. *Rev Esp Med Legal*. 2015;41(03):91-102.

[11] Escario JA, Martínez Quiñones JV, Gallego AM, Arregui Calvo R, Suárez Mier MP. Hernias encefálicas. Clasificación, neuropatología y problemas medicolegales. *Rev Esp Med Legal*. 2015;41(03):91-102.

[12] Mavridis I. Gross and Neurosurgical Anatomy of the Cerebellar Tonsil. *OA Anatomy*. 2014;2(01):8-13.

[13] Luijkx T, Gaillard F. Chiari I malformation. Disponible en: https://radiopaedia.org/articles/chiari-i-malformation. Accedido el 2 de Junio de 2019.

[14] Jiménez-Caballero PE, Fermín-Marrero JA. Cefalea orgasmica secundaria a malformacion de Chiari tipo 1 resuelta tras cirugia descompresiva. *Rev Neurol*. 2014;59(01):47-48.

[15] Barkovich AJ, Wippold FJ, Sherman JL, Citrin CM. Significance of Cerebellar Tonsillar Position on MR. *AJNR Am J Neuroradiol*. 1986; 7(05):795-799.

[16] Furuya K, Sano K, Segawa H, Ide K, Yoneyama H. Symptomatic Tonsillar Ectopia. J *Neurol Neurosurg Psychiatry*. 1998;64(02):221-226.

[17] Aparici F, Menor F, Matí Bonmatí L, Miguel A, Pamies J, Sancho A. Herniación amigdalina en la malformación de Chiari en la edad pediátrica: observación y evolución en el tiempo. *Radiologia*. 2001;43(05):243-248.

[18] Mikulis DJ, Díaz O, Egglin TK, Sánchez R. Variance of the Position of the Cerebellar Tonsils with Age: Preliminary Report. Radiology. 1992;183(03):725-728.

[19] Arana Fernández de Moya E. Demencias e Imagen: lo básico. Radiologia. 2010;52(01):4-17.

[20] Vargas López DA, Rodríguez Alvarez JC. Indice Bicaudado, Indice Bifrontal e Indice de Evans en Tomografías Cerebrales Normales. *Revi Peru de Radiol*. 2008;12(26):27-29.

[21] Factora R, Luciano M. Normal Pressure Hydrocephalus: Diagnosis and New Approaches to Treatment. *Clin Geriatr Med*. 2006;22(03):645-657.

[22] Fatterpekar GM, Dietrich A, Pantano P, Saba L, Knopp EA, Piattella MC, et al. Cerebral Peduncle Angle: An Objective Criterion for Assessing Progressive Supranuclear Palsy Richardson Syndrome. *AJR Am J Roentgenol*. 2015;205(02):386-391.

[23] Warmuth-Metz M, Naumann M, Csoti I, Solymosi L. Measurement of the Midbrain Diameter on Routine Magnetic Resonance Imaging: A Simple and Accurate Method of Differentiating Between Parkinson Disease and Progressive Supranuclear Palsy. *Arch Neurol*. 2001;58(07):1076-1079.

[24] Patro SN, Glikstein R, Hanagandi P, Chakraborty S. Role of Neuroimaging in Multidisciplinary Approach Towards Non-Alzheimer's Dementia. *Insights Imaging*. 2015;6(05):531-544.

[25] Sobrino Guijarro B, Alcazar A, Ordóñez González A, Montoya Bordón J, Alonso Torres A, Lingam R. Revisión radiológica de las causas de proptosis ocular. Disponible en. Accedido el 15 de Junio de 2019.

[26] Nugent RA, Belkin RI, Neigel JM, Rootman J, Robertson WD, Spinelli J, et al. Graves Orbitopathy: Correlation of CT and Clinical Findings. Radiology. 1990;177(03):675-682.

[27] Bell D, Hameed A. Proptosis. Disponible en: https://radiopaedia.org/articles/proptosis-1?lang=us. Accedido el 12 de junio de 2019.

[28] Freitas Soares Machado K, Mattos García M. Thyroid Ophthalmopathy Revisited. *Radiol Bras*. 2009;42(04):261-266.